Diminished metastasis in tetraspanin CD151–knockout mice

Yoshito Takeda,[1] Qinglin Li,[1] Alexander R. Kazarov,[1] Mathieu Epardaud,[1] Kutlu Elpek,[1] Shannon J. Turley,[1] and Martin E. Hemler[1]

[1]Dana-Farber Cancer Institute, Boston, MA

Tetraspanin protein CD151 on tumor cells supports invasion and metastasis. In the present study, we show that host animal CD151 also plays a critical role. CD151-null mice showed markedly diminished experimental lung metastasis after injection of Lewis lung carcinoma or B16F10 melanoma cells. Diminished tumor cell residence in the lungs was evident 6-24 hours after injection. Consistent with an endothelial cell deficiency, isolated CD151-null mouse lung endothelial cells showed diminished support for B16F10 adhesion and transendothelial migration, diminished B16F10-induced permeability, and diminished B16F10 adhesion to extracellular matrix deposited by CD151-null mouse lung endothelial cells. However, CD151 deletion did not affect the size of metastatic foci or subcutaneous primary B16F10 tumors, tumor aggregation, tumor clearance from the blood, or tumor-induced immune cell activation and recruitment. Therefore, the effects of host CD151 on metastasis do not involve altered local tumor growth or immune surveillance. VEGF-induced endothelial cell signaling through Src and Akt was diminished in CD151-null endothelial cells. However, deficient signaling was not accompanied by reduced endothelial permeability either in vitro (monolayer permeability assay) or in vivo (VEGF-stimulated Miles assay). In summary, diminished metastasis in CD151-null host animals may be due to impaired tumor-endothelial interactions, with underlying defects in mouse lung endothelial cell extracellular matrix production. (*Blood*. 2011;118(2): 464-472)

Introduction

Metastasis is the leading cause of cancer-related death. The metastatic process consists of a series of events: tumor cell intravasation, circulation in blood and lymph vasculature, arrest in a distant organ, extravasation, and growth into metastatic foci.[1] Tumor–endothelial cell interactions are particularly important. Not only do tumor cells traverse the endothelium during intravasation and extravasation, but they may also arrest and grow within blood vessels.[2]

Tetraspanins, a family of proteins with specialized features, including 4 conserved transmembrane domains, are found on nearly all cell and tissue types in nearly all types of animals. Tetraspanins function by organizing integrins, membrane-bound growth factors, and other membrane-associated proteins into complexes known as tetraspanin-enriched microdomains (TEMs).[3,4] Tetraspanins can regulate cell morphology, motility, invasion, fusion, protein trafficking, and signaling, thereby influencing immune responses, viral infections, tumor biology, fertilization, hematopoiesis, brain development, and other processes.[5-7]

Tetraspanins regulate multiple steps during tumor progression, including metastasis.[8] For example, expression of CD9/MRP-1, CD82/KAI-1, and CD63/ME491 on tumor cells may suppress metastasis.[9,10] Conversely, metastasis may be enhanced by the tumor-cell tetraspanins CO-029[11] and CD151.[12-14] CD151 is present on nearly all epithelial and endothelial cell types, and is the tetraspanin most closely associated with laminin-binding integrins.[15,16] Therefore, CD151 can modulate integrin $\alpha 3\beta 1$-, $\alpha 6\beta 1$-, and $\alpha 6\beta 4$-dependent neurite outgrowth, cell migration, cell morphology, and adhesion strengthening.[17-20] The capability of CD151 to support tumor-cell invasion and migration helps to explain its positive contribution to metastasis.[12,21]

Although many studies have focused on the functions of tumor-cell tetraspanins, few have addressed the effects of host-animal tetraspanins on tumor progression. We previously demonstrated that mouse *CD151* deletion caused impaired pathologic angiogenesis in Matrigel plug, corneal micropocket, and tumor implantation assays.[22] Although the absence of host CD151 decreased primary tumor growth in one example, we did not examine secondary tumor growth (ie, metastasis) in that study. In the present study, we demonstrate that host CD151 supports experimental lung metastasis by B16F10 melanoma and Lewis lung carcinoma (LLC) cells. The absence of host CD151 minimally affected endothelial permeability and the host immune response to injected tumor cells. However, CD151 removal from host endothelial cells did cause deficiencies in tumor-endothelial adhesion and transendothelial migration, which may explain the diminished tumor metastasis in CD151-null mice.

Methods

CD151-null mice

CD151-null mice, generated as described previously,[22] were backcrossed >7 generations into the C57BL/6J mouse strain, and housed under pathogen-free conditions at the Dana-Farber Cancer Institute. Genotyping of all breeding pairs was confirmed by PCR analysis. In all studies,

Submitted August 17, 2010; accepted April 17, 2011. Prepublished online as *Blood* First Edition paper, May 2, 2011; DOI 10.1182/blood-2010-08-302240.

The online version of this article contains a data supplement.

The publication costs of this article were defrayed in part by page charge payment. Therefore, and solely to indicate this fact, this article is hereby marked "advertisement" in accordance with 18 USC section 1734.

CD151-null mice, 7-12 weeks old, were compared with littermates of the same age and gender. Animal studies were approved by the Dana-Farber Cancer Institute Animal Care and Use Committee.

Cells

Mouse lung endothelial cells (MLECs) were isolated as described previously.[22] Briefly, lung lobes were minced, digested (40 minutes) with 0.2% collagenase (Worthington) at 37°C in DMEM, and then incubated with Dynabeads (Dynal Biotech) coated with anti–mouse CD31 (Pharmingen). Cells on beads were separated with an MPC-1 magnetic separator (Dynal) and then cultured on 0.1% gelatin-coated plates for 5-7 days until confluent. Subconfluent cells were then detached and selected using Dynabeads coated with rat anti–mouse CD102 (ICAM-2; Pharmingen). Isolated MLECs were cultured in DMEM containing 20% FCS, 100 U/mL of penicillin G, 0.1 mg/mL of streptomycin, 2mM L-glutamine, 1× nonessential amino acids, 1× sodium pyruvate, 25mM HEPES, 100 μg/mL of heparin, and 100 μg/mL of endothelial cell growth supplement (Biomedical Technology). Cells were passaged no more than 4 times. Greater than 90% of the cells stained positive for the endothelial cell marker von Willebrand factor (pAb; Dako). Mouse primary keratinocytes were isolated and cultured as described previously[23] and were used within 2-3 days. The murine B16F10 and LLC cell lines, histocompatible with C57BL/6J mice, were cultured in DMEM containing 10% FCS. Tumor cell viability was $> 95\%$, as shown by Trypan Blue exclusion.

Flow cytometry

Flow cytometry was performed as described previously.[22] MLECs were incubated with primary Abs for 1 hour at 4°C, washed with PBS twice, and then incubated with FITC-conjugated secondary antibody. After washing again with PBS, cells were resuspended in 4% paraformaldehyde and acquired using CellQuest software (1997 version). Negative control peaks were obtained using secondary antibody alone. Monoclonal antibodies to mouse CD9 (KMC8), CD81 (Eat1), CD44 (KMI 114), α5 (5H10-27), α6 (GoH3), αv (H92B8), β1 (9EG7), ICAM-1 (YN1/1.7.4), and VCAM-1(429) were all from BD Biosciences.

In vivo tumor experiments

For local tumor growth, 1×10^6 B16F10 cells were injected subcutaneously as described previously.[22] Tumors were measured every 5 days and the volume was calculated (length × width^2 × 0.52). After 15 days, tumors were collected and weighed. For lung experimental metastasis, B16F10 melanoma cells and LLC cells were trypsinized, resuspended in PBS, and then 1×10^6 cells (in 0.2 mL) were injected via the lateral tail vein using a 27-gauge needle. Mice were killed 14 days after injection and tissues were isolated and fixed in 10% neutral-buffered formalin, injected under 25 cm of aqueous pressure. Lungs containing LLC metastases were immersed in Bouin solution to distinguish white tumor colonies from yellowish lung parenchyma. Surface metastatic foci in lung left lobes were counted under a dissecting microscope. For quantitation of metastatic nodule size, photos of random fields were obtained (using a low-magnitude 2× lens), and then the sizes of at least 20 nodules were determined using NIH Image software (Version 1.44) and averaged.

In some experiments, B16F10 and LLC cells were labeled for 30 minutes with 2′,7′-bis-(2-carboxyethyl)-5-(and-6)-carboxyfluorescein, acetoxymethyl ester (BCECF-AM; Molecular Probes), washed twice, and injected as in the previous paragraph. After 6 hours, mice were killed, and surface metastatic loci in the left lobes of the lung were counted using a fluorescence microscope; alternatively, cryosections were prepared and metastatic loci were visualized. In other experiments, B16F10 cells were labeled with the cell-permeable fluorescent dye CFSE (Invitrogen). Cells ($0.5\text{-}1 \times 10^6$ in 200-300 μL of PBS) were then injected slowly (~ 2 minutes per injection to prevent clumping). Control mice were injected with PBS only. After 24-72 hours, mice were killed and blood samples were collected directly from the heart into tubes containing 10mM EDTA in PBS to prevent coagulation and erythrocytes were lysed. Mice then were perfused with 20 mL of PBS with 2mM EDTA until the lungs and liver appeared white. After perfusion, lungs were collected and processed by gentle mechanical disruption with forceps, followed by enzymatic digestion using RPMI with 1 mg/mL of collagenase D (Roche), 0.8 mg/mL of dispase (Invitrogen), and 0.1 mg/mL of DNase I (Sigma). Tissue suspensions (5-6 mL per lung) were incubated at 37°C for 45 minutes with vigorous pipetting every 15 minutes to help tissue digestion. After cells were strained with 70-μm nylon mesh, they were suspended in PBS with 5% FBS and 2mM EDTA (FACS buffer) and Fc receptors were saturated using FcR-block antibody (2.4G2). Cells were then stained with fluorescently labeled monoclonal antibodies for CD45 (30-F11) and 7-amino-actinomycin D, a nucleic acid dye for staining of apoptotic cells, at 4°C for 30 minutes, washed in FACS buffer, and analyzed immediately using FACSCalibur (BD Biosciences). Data were analyzed using FlowJo software (Version 8.7.3).

Tumor adhesion assays

MLECs or keratinocytes were plated on 0.1% gelatin-coated 96-well microplates, allowed to form a monolayer for 3 days, and incubated with or without 50 ng/mL of TNF-α. To measure adhesion, melanoma cells were labeled for 30 minutes with BCECF-AM, and then 3×10^4 cells (in 0.2 mL) were added to each well containing endothelial cell monolayers or control keratinocyte monolayers. After 30 minutes at 37°, plates were washed 3 times with warm PBS and adherent cells were quantitated using a Cytofluor 2300 device (Millipore).

Other adhesion experiments used crude extracellular matrix (ECM) synthesized by MLECs or mouse keratinocytes. Briefly, cells were cultured for 3 days in 96-well tissue-culture plates, then removed by sequential washing with 1% (vol/vol) Triton X-100 in PBS, followed by 2M urea in 1M NaCl. Washing solutions contained protease inhibitors (1mM PMSF and 2mM N-ethylmaleimide). Finally, plates were washed with PBS, incubated with 1% BSA, and then used in melanoma adhesion assays as described in the previous paragraph.

Transendothelial migration

MLECs or control keratinocytes were plated in the upper chambers of polycarbonate filter wells (Transwell, 8-μm pores; Costar plates; Corning) coated with 0.1% gelatin. After monolayers were formed (~ 3 days), calcein-labeled B16F10 (1×10^5 cells in 200 μL of DMEM and 1% FCS) were added to upper chambers and incubated for 3 and 12 hours at 37°C. Lower chambers contained 700 μL of DMEM with 10% FCS. B16F10 cells migrating through monolayers of MLECs or keratinocytes and attaching to the undersides of filters were counted in triplicate wells with aid of an Eclipse TE300 inverted fluorescence microscope (Nikon) using a 20× objective.

In vitro and in vivo permeability assays

To assess endothelial cell permeability, MLEC monolayers were formed in the upper chambers of Transwells (0.4-μm pores), and then FITC-dextran (40S; Sigma-Aldrich) was added (at 1 mg/mL) for the indicated times and FITC-dextran passing through to the lower chambers was quantitated by fluorometry (absorption/emission at 492/520 nm). To assess tumor-induced endothelial cell permeability, B16F10 (1×10^5 cells in 200 μL of DMEM) was added together with FITC-dextran, and 70μL of medium from the lower chambers was collected and FITC-dextran was quantitated.

In vivo permeability was assessed using a modified Miles assay. Briefly, Evan Blue dye (Sigma-Aldrich) was injected into mouse tail veins (200 μL of 0.5% solution in PBS). After 10 minutes, 25 μL of PBS (with or without 60 ng of mouse $VEGF_{165}$) was injected intradermally. One hour later, shaved dorsal skin at the injection area was excised, weighed, extracted with formamide for 4 days, and dye was measured at 610 nm.

Signaling assays

MLECs were seeded onto plates previously coated with Matrigel (diluted 1:30). After cells reached confluence, they were incubated in low serum (DMEM containing 0.5% FBS) for 12 hours, stimulated with VEGF (20ng/mL) for various times, and then lysed in buffer containing 1% NP-40. Equal amounts of proteins were resolved by SDS-PAGE, transferred to

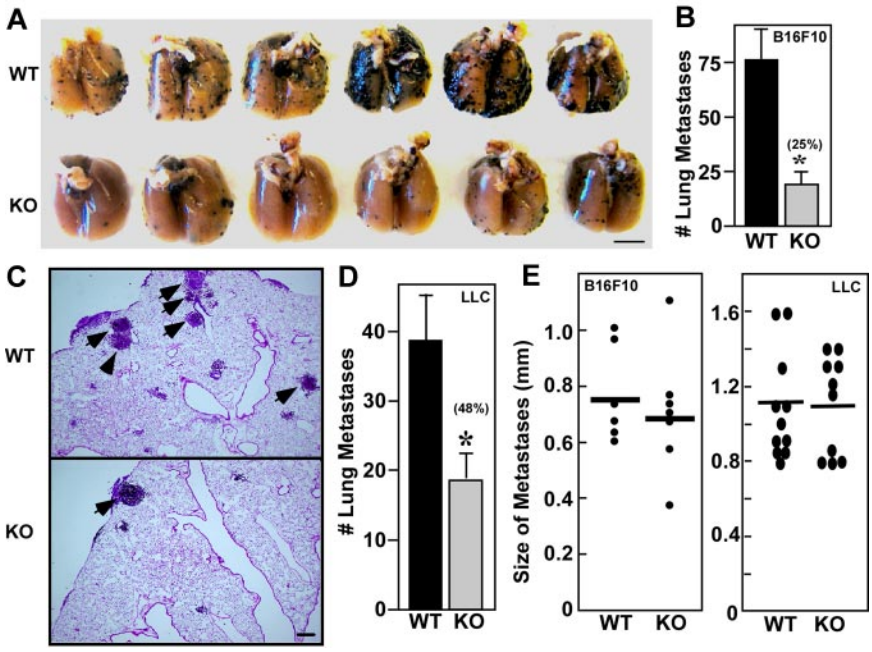

Figure 1. Host CD151 affects experimental pulmonary metastasis. (A) Representative photograph of pulmonary metastatic foci produced 14 days after intravenous injection of B16F10 cells. Scale bar indicates 5 mm. (B) Numbers of experimental pulmonary B16F10 metastases in left lobes. (C) Representative lung H&E sections of metastases from wild-type (WT) and CD151-null (KO) mice. Arrows point to metastatic foci. Scale bar = 200 μm. (D) Numbers of experimental pulmonary metastasis formed by LLC cells (n = 5). (E) Size distributions of B16F10 and LLC metastatic foci. Data are representative of 3 independent experiments with similar results. Error bars indicate means ± SEM.

nitrocellulose membranes, and then immunoblotted. Anti–phospho-Akt (Ser473), anti-Akt, anti–phospho-p38 (Thr180/Tyr182), anti-p38, anti–phospho-Src (Thy416), anti–phospho-FAK (Tyr925), and anti–phospho-Erk (Thr202/Tyr204) were from Cell Signaling Technology and anti–c-Src was from Santa Cruz Biotechnology.

Immune cell assays

To assess dendritic cell (DC) migration, mice were anesthetized with Avertin (2.5% tribromoethanol) and then 25 μL of 0.8% FITC isomer 1 (Sigma-Aldrich) dissolved in 1:1 acetone:dibutylphthalate was painted onto shaved abdominal skin at the level of the inguinal lymph node. After 24 hours, draining and contralateral inguinal lymph nodes were harvested. The percentages of DCs expressing and not expressing FITC were determined by 2-color flow cytometry using PE-conjugated monoclonal antibody against CD11c (Becton Dickinson).

We also analyzed antigen presentation by DCs. To obtain an enriched BM-DC population, total mouse BM cells were cultured for 5 days in complete medium (RPMI containing 10% FBS, 0.5% glutamate, and 0.1% β mercaptoethanol) supplemented with 3% GM-CSF. BM-DCs were then pulsed for 2 hours with 100 μg/mL of OVA and cocultured at different concentrations with 1×10^6 CFSE-labeled OT-I cells (OVA-specific CD8 T cells) for 60 hours. In addition, pulsed BM-DCs were cocultured with 3×10^5 CFSE-labeled OT-II cells (OVA-specific CD4 T cells) for 60 hours. After coculture, OT-I and OT-II cells were labeled with allophycocyanin-conjugated monoclonal antibody against the Vα2 chain (which is expressed by OT-I and OT-II T cells) and with peridinin chlorophyll A protein–conjugated monoclonal antibody against CD8α or CD4, respectively. Dual antibody–labeled cells were analyzed by flow cytometry, and CFSE dilution was assessed to measure OT-I or OT-II proliferation.

We also injected mice intravenously with B16F10 melanoma cells, waited 15 days, and then collected spleens, lungs, and lung-draining lymph nodes. Single-cell suspensions were prepared from these tissues, and immune cell subsets were analyzed using 4-color flow cytometry.

Microscopy and image acquisition

Images in Figure 1A and supplemental Figure 8A (available on the *Blood* Web site; see the Supplemental Materials link at the top of the online article) were acquired using a digital camera. The Figure 1C image was acquired using a monochrome CCD camera (Spot RT; Diagnostic Instruments) on an Axiovert 135 inverted microscope (Zeiss). Images in Figure 2A, Figure 5A, Figure 6A, supplemental Figure 2A, supplemental Figure 5A, and supplemental Figure 6A were obtained using an Eclipse TE300 inverted microscope (Nikon) equipped with a 2× objective (for Figure 2A and supplemental Figure 2A), a 10× objective (for Figure 5A and supplemental Figures 5A and 6A), or a 20× objective (used for Figure 6A) and an RT Monochrome SPOT camera (Diagnostic Instruments) and then analyzed with Scion Image software (Version 4.0.3.2). All photos were processed (cropped, labeled, and organized) for publication using Canvas version 9.0 software (ACD Systems).

Results

Host CD151 affects experimental lung metastasis

B16F10 melanoma cells were injected into mouse tail veins and experimental lung metastasis was evaluated. Two weeks later, there were significantly fewer metastatic foci in the lungs of CD151-null mice compared with wild-type mice (Figure 1A-B). These experiments used CD151-null mice backcrossed into C57BL/6 mice for > 7 generations. In a mixed background (C57BL/6 and 129SvEv), B16F10 lung metastasis was also markedly diminished for CD151-null mice compared with their wild-type littermate controls (not shown). Detailed microscopic analysis of lung tissue sections consistently revealed larger numbers of metastatic foci in the lungs of wild-type mice (Figure 1C). Metastatic foci in both groups were distributed as perivascular and subpleural lesions. The absence of infiltrating leukocytes is consistent with the absence of an antitumor immune response in both types of mice (Figure 1C). We also injected LLC cells and examined experimental lung metastasis, and, again, there was a significant decrease in the number of metastatic nodules in lungs of CD151-null mice compared with wild-type mice (Figure 1D). B16F10 cells also metastasized to other organs in addition to the lungs. Among 6 wild-type mice, metastases appeared in the kidney (1 of 6), peritoneum (4 of 6), and ovary (2 of 6). In contrast, CD151-null mice showed 0 of 6, 2 of 6, and 1 of 6 metastases in these tissues, respectively. Although larger numbers are needed, the trend seems to be toward diminished

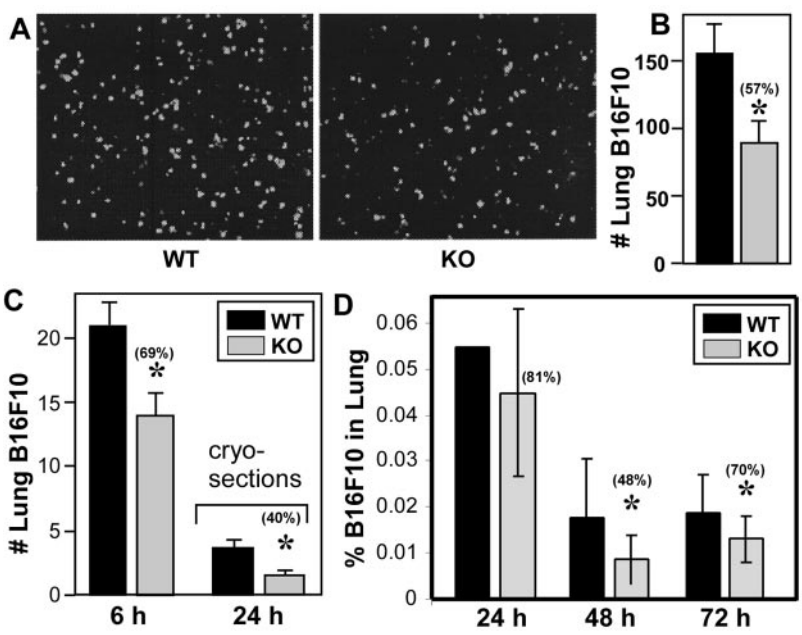

Figure 2. Host CD151 affects lung localization. (A) Representative photos of fluorescent B16F10 cells (labeled with BCECF-AM) in lungs 6 hours after tail vein injection. (B) Quantitation of fluorescent B16F10 cells in lung left lobes (n = 5). (C) In a separate experiment, fluorescent B16F10 cells were again injected and after 6 hours were counted in whole-lung left lobes (left bars; n = 5) or after 24 hours in cryosections at higher magnification (right bars; n = 5). (D) B16F10 cells labeled with CFSE were injected into mouse tail veins. After 24-72 hours, mice were killed, perfused, lungs were digested, and the percentage of CFSE-labeled cells (relative to total suspended lung cells) was determined using flow cytometry. Error bars indicate means ± SEM. *$P < .05$. WT indicates wild-type; KO, knockout.

metastasis in CD151-null mice. Size distributions of individual B16F10 and LLC metastatic foci were not significantly different between the 2 mouse genotypes (Figure 1E), suggesting that local growth was unperturbed. To further assess local growth effects, B16F10 melanoma cells were injected subcutaneously into the dorsal flanks of wild-type and CD151-null mice. At the indicated times, tumor volumes (supplemental Figure 1A) and weights (supplemental Figure 1B) were indistinguishable. Moreover, histologic analyses revealed no difference in microvascular density within these tumors (data not shown).

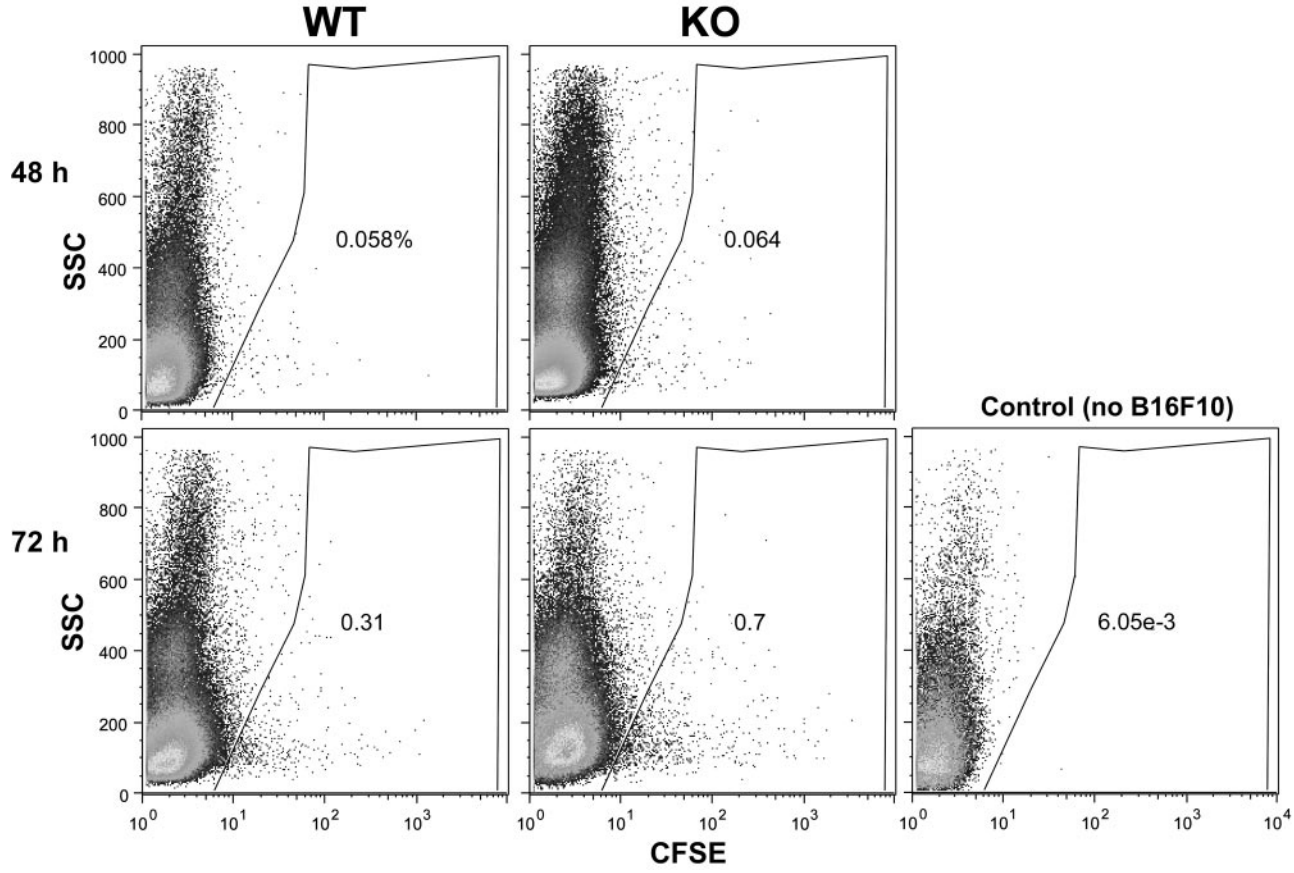

Figure 3. B16F10 cells in blood. B16F10 cells labeled with CFSE were injected into mouse tail veins. After 48-72 hours, blood samples were collected directly from the heart and the percentage of CFSE-labeled cells was determined by flow cytometry. Note that blood from a control mouse (no B16F10 injection) contained essentially no CFSE-labeled cells. SSC indicates side scatter; WT, wild-type; KO, knockout.

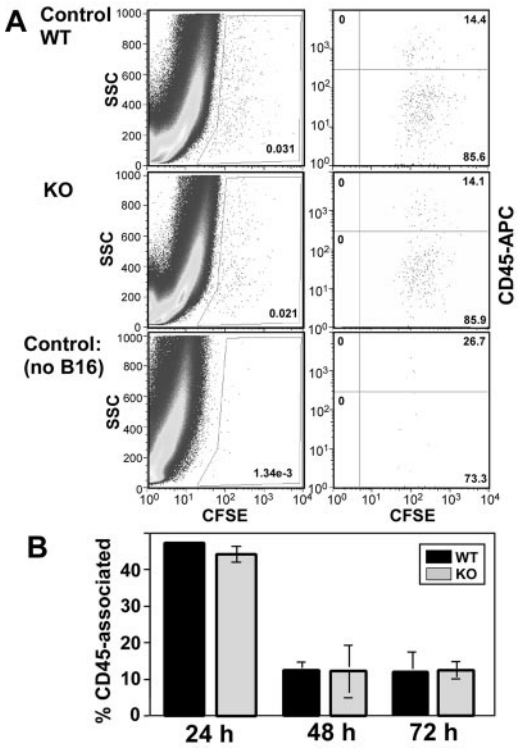

Figure 4. B16F10 cells associated with leukocytes in lungs. B16F10 cells labeled with CFSE were injected into mouse tail veins. (A) After 48 hours, lungs were digested and analyzed for presence of CFSE-B16F10 as in Figure 2D (left panels). In addition, $CFSE^+$ cells (gated as in left panels) were stained with CD45-allophycocyanin (anti-CD45 monoclonal antibody conjugated with allophycocyanin; right panels). Note that $CFSE^+$ cells were essentially absent in the sample from a control mouse with no B16F10 injection (bottom panels). (B) $CFSE^+$ cells from digested lung cell preparations were analyzed to determine the percentage of CD45-associated cells (as in panel A). Error bars indicate means ± SEM. WT indicates wild-type; KO, knockout.

B16F10 distribution and clearance at early time points

To gain insight into why metastases were diminished in C151-null mice, B16F10 and LLC distribution was examined at early time points. Equal numbers of fluorescently labeled B16F10 cells were injected into CD151-null and wild-type mouse tail veins, and 6 hours later, lungs were isolated and fluorescent cells on their surfaces were visualized (Figure 2A) and quantitated (Figure 2B). In this experiment and in another 6-hour experiment (Figure 2C), CD151-null mouse lungs contained significantly fewer B16F10 cells, as seen on lung surfaces and/or in cryosections. Similarly, fewer LLC cells were seen on the lung surfaces of CD151-null mice after 6 hours (supplemental Figure 2A-B). For 24- to 72-hour analyses, lungs were perfused, digested to prepare single-cell suspensions, and then the relative percentage of CFSE-labeled B16F10 cells was determined (Figure 2D). Significantly fewer B16F10 cells were recovered from CD151-null mice at 48 and 72 hours, and a similar trend was seen at 24 hours.

Next we considered that rapid clearance from the blood could potentially result in fewer B16F10 cells being available for lung colonization in CD151-null mice. However, the percentage of CFSE-positive B16F10 cells was not diminished in the blood of CD151-null mice at either 48 or 72 hours (Figure 3). Furthermore, the relative size distributions (indicated on y-axes) for B16F10 cells from CD151-null mice were not altered. Therefore, B16F10 cells in the blood of CD151-null mice did not appear to differentially assemble into larger aggregates (eg, with leukocytes and/or platelets). B16F10 cells isolated from the lungs were also not differentially aggregated, as evidenced by similar 48-hour size profiles seen for CD151-negative and CD151-positive mice (Figure 4A left panels). A subset of lung-derived B16F10 cells (~14%) was engaged with leukocytes, as seen by CFSE and CD45 double staining after 48 hours (Figure 4A right panels). However, leukocyte engagement with B16F10 cells did not differ between CD151-null and CD151-positive host mice at 24, 48, or 72 hours (Figure 4A-B). In addition, lung-derived CFSE-positive cells did not show an increased tendency to undergo cell death in CD151-null mice, as seen by 7-amino-actinomycin D staining (supplemental Figure 3).

Assessment of tumor immunity

Recruitment of cytotoxic cells, such as $CD8^+$ T cells and natural killer (NK) cells, can affect the tumor burden in the lung.[24,25] Therefore, after B16F10 injection, we looked for changes in the composition of immune cell subsets. We digested total lung, spleen, and lung-draining lymph nodes from CD151-null and wild-type tumor-bearing mice, and then quantitated cells expressing the surface markers CD4, CD8, CD11c, NK1.1, and B220. Relative immune cell percentages from spleen, lung, and lung-draining lymph nodes were not significantly different between CD151-null and wild-type mice (Table 1). Because DCs contribute to tumor immunity, we investigated the migration of DCs from the skin to draining lymph nodes after FITC painting of mouse flanks. However, CD151-null and wild-type mice did not differ in numbers of FITC-labeled and CD11c-positive DCs identified in the draining and contralateral inguinal lymph nodes (Table 2). Because DCs participate in tumor surveillance and can be affected by CD151 ablation,[26] we also examined DC function in a model antigen-presentation system. Antigen-pulsed DCs derived from the BM of CD151-null and wild-type mice were incubated with antigen-specific CD4 and CD8 T-cell clones. CD151-null and wild-type-derived DCs were not different with respect to induction of antigen-specific T-cell proliferation (Table 3).

Endothelial cell CD151 promotes B16F10 adhesion and transendothelial migration

With no evidence for alterations in B16F10 clearance, growth, apoptosis, leukocyte interactions, or immune system activation, we focused on B16F10 interactions with endothelial cells. In the multistage metastatic cascade, tumor-endothelial cell interaction is particularly important, with lung metastasis initiated by intravascular attachment to the endothelium.[2] We conducted tumor-endothelial adhesion assays to explore possible endothelial cell CD151 effects on the initial adhesion of B16F10 melanoma cells.

Table 1. Relative percentages of leukocytes from $CD151^{+/-}$ and $CD151^{-/-}$ mice injected IV with B16F10 melanoma cells

		Relative % to total cells*				
Tissue	Genotype	CD4	CD8α	CD11c	NK1.1	B220
Spleen	$CD151^{+/-}$	19.0	13.7	1.7	11.0	37.6
	$CD151^{-/-}$	16.6	13.1	1.4	12.2	39.4
Lung	$CD151^{+/-}$	2.2	1.7	7.3	13.7	ND
	$CD151^{-/-}$	1.2	1.3	5.6	12.3	ND
Lung-draining LN	$CD151^{+/-}$	29.7	23.9	0.4	ND	ND
	$CD151^{-/-}$	32.1	28.5	0.3	ND	ND

*From mice injected with B16F10 melanoma cells, the indicated tissues were isolated and dispersed. Relative to the total cells analyzed, the percentages of $CD4^+$ and $CD8^+$ T cells, $CD11c^+$ DCs, $NK1.1^+$ NK cells, and $B220^+$ B cells were determined by flow cytometry.

LN indicates lymph nodes; and ND, not determined.

Table 2. CD151 effects on skin DC migration from the abdomen to draining lymph nodes

Genotype	DCs*	FITC + DCs†
CD151$^{+/+}$	10.0%	58.3%
CD151$^{+/-}$	8.6%	50.1%
CD151$^{-/-}$	12.3%	58.5%

*Percentage of total lymph node cells analyzed.
†Percentage of CD11c^{+} cells also containing FITC.

After 30 or 90 minutes, B16F10 melanoma cells adhered significantly less to representative monolayers of MLECs derived from CD151-null mice (Figure 5A-B). After the addition of TNF-α, which up-regulates adhesion molecules on endothelial cells, a significant difference between CD151-null and wild-type endothelial cells was maintained (Figure 5B). In addition, fluorescently labeled B16F10 cell spreading (~ 5% on CD151-null cells) was diminished compared with wild-type cell spreading (~ 50%; Figure 5A). We considered that CD151-null endothelial cells might express diminished levels of molecules involved in cell adhesion, spreading, and/or migration. However, the amounts of adhesion molecules (β1 integrin subunit, VCAM-1, and ICAM-1) were indistinguishable between CD151-null and wild-type endothelial cells, either in the presence or absence of TNF-α, as determined by flow cytometry (supplemental Figure 4). Also unchanged were expressions of CD44, the tetraspanins CD9 and CD81, and the integrin subunits α5, α6, and αV (not shown).

The presence of extracellular laminin matrix interposed between tumor cells and endothelial cells can play a role in the formation of micrometastases.[27] Furthermore, CD151-null mice showed disorganized laminin ECM organization during wound healing.[28] Therefore, defective ECM production by CD151-null endothelial cells might account for diminished B16F10 adhesion. Endothelial cells were plated and removed, and the underlying ECM was tested for its ability to support B16F10 adhesion. ECM derived from CD151-null mice supported significantly less B16F10 adhesion (Figure 5C). BSA coating alone did not support tumor attachment (not shown). These results indicate a marked functional deficiency in the ECM produced by CD151-null endothelial cells.

Tumor cell extravasation involves transendothelial migration, which can be rate limiting during the metastatic cascade. Therefore, we performed B16F10 transendothelial migration assays to assess the involvement of CD151. Transendothelial migration of B16F10 through monolayers of CD151-null endothelial cells was markedly diminished, as seen in representative images showing fluorescently labeled B16F10 melanoma cells (Figure 6A). Quantitation of results from multiple experiments after transendothelial migration for 3 or 12 hours consistently revealed a significant deficit in migration through CD151-null monolayers (Figure 6B). Because attached tumor cells can facilitate tumor extravasation by causing endothelial cell retraction, we performed a tumor cell–induced endothelial retraction assay.[29] After incubation with B16F10 cells, CD151-null endothelial cells showed a modest but significant decrease in FITC-dextran permeability (Figure 6C).

In control experiments, B16F10 cells were tested for adhesion to confluent mouse keratinocytes (supplemental Figure 5A-B), adhesion to ECM deposited by keratinocytes (supplemental Figure 5C), and transmigration through a confluent monolayer of keratinocytes (supplemental Figure 6A-B). In each case, CD151 wild-type and mouse keratinocytes showed negligible differences. Therefore, the effects of CD151 ablation differ sharply between endothelial cells and keratinocytes.

VEGF effects on endothelial cells

VEGF is a potent inducer of endothelial cell hyperpermeability.[30] Therefore, we speculated that CD151 could affect lung metastasis by modulating endothelial responses to VEGF. Endothelial cell stimulation by VEGF affects several signaling molecules, including Src, Akt, p38 MAPK, ERK, and FAK.[31,32] As shown in supplemental Figure 7, phosphorylation of Src was markedly attenuated in CD151-null MLECs compared with wild-type MLECs after stimulation with VEGF. Phosphorylation of Akt was also diminished, but phosphorylation of ERK and p38 MAPK was minimally altered (supplemental Figure 7), and FAK phosphorylation was unchanged (not shown).

Because CD151 affected the endothelial response to VEGF, and because VEGF is a major inducer of vascular permeability, we investigated whether CD151 affects the VEGF-induced endothelial cell monolayer permeability using a Miles assay. This assay assesses leakage of Evan Blue dye into intradermal sites after injecting with factors such as VEGF that may increase permeability. As shown in supplemental Figure 8A-B, the intensity of dye staining was indistinguishable between CD151-null and wild-type mouse skin samples after intradermal injection with either control PBS or VEGF. We also investigated vascular permeability to FITC-dextran in a standard in vitro assay, and CD151-null and wild-type cells did not differ significantly in either 1- or 3-hour assays in the absence or presence of TNFα (supplemental Figure 8C) or VEGF (supplemental Figure 8D).

Discussion

Studies linking CD151 with metastasis[12-14] have so far focused on tumor cell CD151. In the present study, we demonstrated that host-animal CD151 can also play a key role in supporting metastasis. When either B16F10 melanoma or LLC cells were injected into the tail veins of CD151-null mice (of either the C57BL/6J or the Sv129 strain), experimental lung metastasis was markedly curtailed. Preliminary results also showed a trend toward diminished metastasis in other organs (ie, the kidney, peritoneum, and ovary).

Because inhibition of angiogenesis can also inhibit lung metastasis,[33] and because CD151-null mice are deficient in pathologic angiogenesis,[22] we considered that defective angiogenesis might explain the diminished metastasis in CD151-null mice. However, CD151-null mice did not show smaller metastatic foci after injection of either B16F10 or LLC cells. Furthermore, subcutaneously injected B16F10 cells did not form smaller primary tumors and did not show decreased microvascular density within those tumors. Therefore, defective angiogenesis does not appear to limit local growth of B16F10 cells in metastatic foci or anywhere else in

Table 3. Antigen-specific activation of CD4 and CD8 T cells by BM-DCs from CD151$^{+/-}$ and CD151$^{-/-}$ mice

	OT-I cells dividing		OT-II cells dividing*
	1:150 DCs:T cells	1:75 DCs:T cells	1:50 DCs:T cells
CD151$^{-/-}$	51.2%†	57.2%	14.4%
CD151$^{+/-}$	44.6%	54.7%	15.5%

*OT-I and OT-II are OVA-specific CD4 and CD8 T cells that were isolated from TCR-transgenic mice.
†DCs from CD151$^{-/-}$ and CD151$^{+/-}$ mice were incubated in vitro (at different DC:T cell ratios) with OVA-specific T cells, and then the percentage of divided cells was determined by flow cytometric quantitation of CFSE dilution.

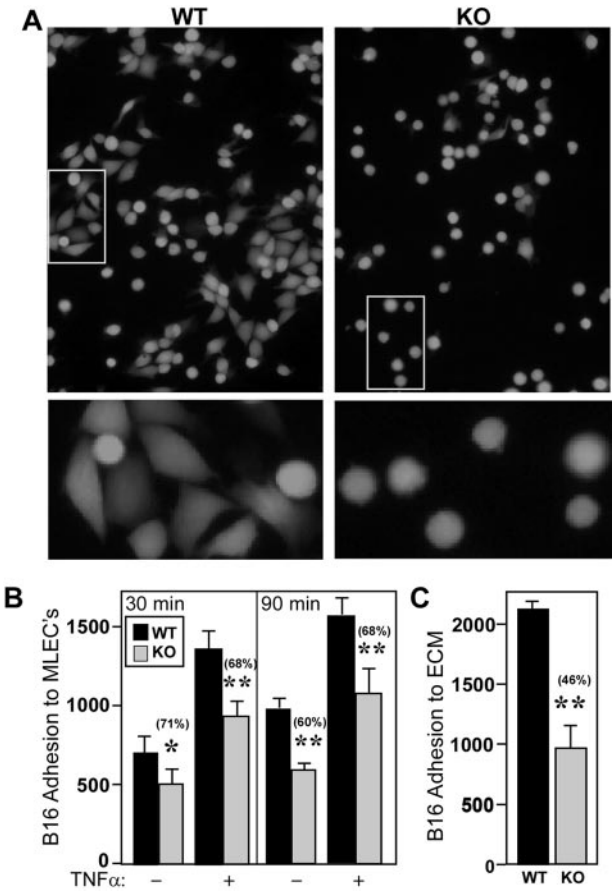

Figure 5. CD151 deletion from endothelial cells affects B16F10 adhesion. (A) Fluorescently labeled B16F10 cells were allowed to adhere to monolayers of wild-type (WT) and CD151-null (KO) MLECs. Representative photos after 90 minutes are shown. White boxes (top panels) are shown at higher magnification in the lower panels. (B) B16F10 adhesion was quantitated after 30 and 90 minutes with or without TNF-α (50 ng/mL; n = 4). $*P < .05$; $**P < .005$. Note that monolayer integrity for CD151-null and wild-type MLEC cells was essentially identical, as evidenced by (1) similar morphology, adhesion, spreading, and migration on gelatin[22]; (2) similar FITC-dextran permeability through monolayers (supplemental Figure 8C-D); and (3) similar electrical resistance, as measured using an electric cell-substrate impedance sensing device (data not shown). (C) Endothelial cell monolayers were removed, and then B16F10 was allowed to adhere for 30 minutes to ECM that had been deposited by either wild-type or CD151-null endothelial cells (n = 4). $**P < .0005$. Data are representative of 3 independent experiments with similar results. Error bars indicate means ± SEM.

CD151-null mice. Instead, we suspect that fewer metastatic foci appear in CD151-null mice due to diminished B16F10 localization into the lung. At early time points (6-72 hours after injection) in 3 different types of assays, fewer B16F10 cells were retained in the lungs of CD151-null mice, although similar numbers were present in the blood. LLC cells also showed a trend toward diminished 6-hour lung retention in CD151-null mice. Therefore, impaired metastasis could result from deficient tumor cell adhesion to lung capillaries and/or from reduced tumor extravasation. Indeed, in vitro assays showed that CD151-null MLECs were deficient in supporting tumor-endothelial adhesion, tumor-transendothelial migration, and tumor-induced permeability to FITC-dextran. By being present at both tumor-endothelial contact sites and endothelial-endothelial junctions,[18,19] CD151 is well positioned to modulate these functions. Consistent with our results, endothelial CD151 was also shown to support lymphocyte interactions with endothelial cells (ie, transendothelial migration and resistance to detachment).[34]

ECM deposited by CD151-null endothelial cells was deficient in supporting B16F10 adhesion, possibly due to defective laminin. First, manipulation of CD151 has been shown to selectively affect cell interactions with laminin compared with other ECM proteins.[22] Second, CD151-null mice were shown to produce disorganized laminin matrix in a skin wound–healing model.[28] Third, laminins were shown to be major components within the ECM produced by endothelial cells.[35] If a disorganized laminin matrix can be associated with delayed wound healing,[28] then disorganized laminin may lead to reduced metastasis. In this regard, laminin matrix interposed between tumor cells and endothelial cells can affect micrometastasis formation.[27] Unfortunately, extensive experimentation with many different anti-mouse laminin antibody preparations failed to yield definitive insights into altered laminin quantity or organization in either lungs or ECM produced by MLECs.

Although B16F10 melanoma cells are syngeneic to C57BL/6 mice, immune cells (eg, T cells, NK cells, and DCs) can be mobilized against injected B16F10 cells.[25,36,37] Because CD151 can regulate the functions of T cells and DCs,[26,38] we considered that alterations in immune cells could underlie the effects of CD151 gene deletion on B16F10 metastasis. However, in CD151-null mice, we saw no appreciable changes in DC activation of T cells or DC trafficking to lung-draining lymph nodes. Furthermore, immune cell subsets (CD4 cells, CD8 cells, DCs, NK cells, and B cells) were not perturbed in B16F10-injected mice, and there was no detectable histological difference in immune cell recruitment to tumor sites. In addition, B16F10 cells in the blood of CD151-null mice were neither more rapidly cleared nor more aggregated, and B16F10 cells isolated from the lungs were neither more associated

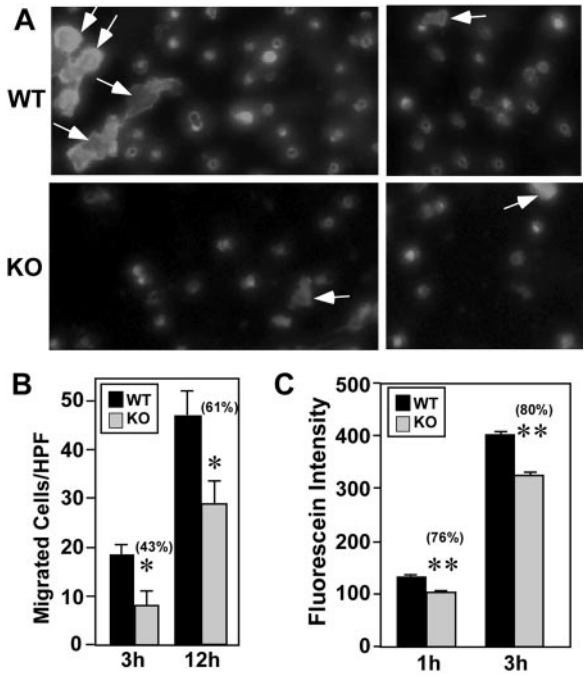

Figure 6. CD151 deletion from endothelial cells affects B16F10 transendothelial migration. (A) Fluorescently labeled B16F10 melanoma cells migrated (12 hours) through wild-type (WT) and knockout (KO) endothelial cell monolayers. Representative photos (2 for each condition) are shown. All fluorescent cells shown had already transmigrated and emerged through the porous filter. Some of these cells, indicated by arrows, had also undergone substantial spreading. (B) After transendothelial migration (for 3 or 12 hours), labeled B16F10 cells were counted using a fluorescent microscope (n = 4). $*P < .05$. (C) After the addition of B16F10 melanoma cells, dextran-FITC permeability through MLEC monolayers was determined (n = 4). $**P < .005$. Data are representative of 3 independent experiments. Error bars indicate means ± SEM.

with leukocytes nor more apoptotic. Therefore, altered immune cell functions do not appear to explain the decreased metastasis in CD151-null mice.

Our results showed that CD151 deletion did not change the expressions of ICAM-1, VCAM-1, integrins, CD44, CD9, or CD81 on endothelial cells, and in a previous study also did not affect integrin expression or activation on several different cell types.[21,22,38-40] Nonetheless, CD151 deletion could still affect the functions of those adhesion molecules. Within endothelial cell docking structures, CD151 associates with VCAM-1,[41] and thus may support VCAM-1–dependent adhesive functions, which play a major role during melanoma adhesion and metastasis.[42] In addition, CD151 associates with laminin-binding integrins (eg, $\alpha3\beta1$, $\alpha6\beta1$, $\alpha6\beta4$, and $\alpha7\beta1$),[16] thereby recruiting the integrins into multicomponent complexes known as TEMs.[3,4] After deletion of CD151 from MLECs, links are disrupted between laminin-binding integrins and at least 5 other proteins.[22] This helps to explain how CD151 modulates laminin-binding integrin-dependent adhesion, adhesion strengthening, neurite outgrowth, migration, and signaling functions.[17-20] Other studies have demonstrated a role for various isoforms of laminin and/or laminin-binding integrins in the regulation of tumor-cell metastasis.[27,43,44] However, it is not yet clear which particular CD151-integrin–laminin complexes are most relevant during B16F10 metastasis.

Vascular permeability is regulated by endothelial nitric oxide synthase and by VEGF signaling through Src and Akt.[31,32,45] CD151 deletion was shown previously to impair adhesion-dependent activation of endothelial nitric oxide synthase[22] and the current results demonstrated VEGF-dependent MLEC signaling through Src and Akt. Therefore, it was surprising that the absence of CD151 did not affect resting or growth factor–induced permeability of an MLEC monolayer in vitro or VEGF-induced skin vascular permeability in vivo. Instead, diminished VEGF-stimulated Src and Akt signaling may be more relevant to impaired endothelial cell migration and angiogenesis, as was seen previously.[22]

Although VEGF stimulates many endothelial cell signaling pathways, deletion of CD151 mostly affected VEGF signaling through Src and Akt, but not FAK or ERK, and only minimally affected p38 MAPK. The molecular basis for highly selective effects of CD151 on endothelial cell signaling, as seen in the present study (supplemental Figure 7) and previously,[22] is unknown. We suspect that CD151 organizes, in the context of TEMs, key molecules that are upstream of Src and Akt during VEGF signaling. It also remains to be determined why in the present study, CD151 deletion affected VEGF-stimulated Src activation in cells that were previously plated on laminin (supplemental Figure 7), but did not affect Src activation in cells newly adherent to laminin in a previous study.[22]

Because CD151 and associated integrins may promote cell migration by enhancing the production of matrix metalloproteinase 9 (MMP-9)[46] and MMP-2,[47] they could also affect metastasis. Indeed, host-derived MMP-2 and MMP-9 can play contributing roles during tumor metastasis to the lungs.[48,49] However, when we compared lung homogenates or MLEC preparations between wild-type and CD151-null mice, we observed no differences in MMP-2 or MMP-9 production or activation, as assessed by gelatin zymogram experiments (Takeda et al[22] and data not shown). Altered platelet function could also play a role in causing diminished metastasis in CD151-null mice, because platelets can contribute to metastasis[50] and because platelets from CD151-null mice have diminished aggregation and spreading functions.[38] However, the absence of diminished B16F10 aggregation within CD151-null mice argues against a role for platelets. This issue will need to be addressed in future studies.

In conclusion, we show that host tetraspanin protein CD151 substantially contributes to lung metastasis by a mechanism likely involving altered tumor-endothelial interactions. Previous studies suggested that CD151 supports metastasis when present on tumor cells.[12-14] Other studies indicated that CD151 contributes to pathologic angiogenesis in mice.[22] Therefore, CD151 is emerging as a potentially useful molecule for which therapeutic targeting may affect multiple steps in tumor progression.

Acknowledgments

We thank Dr R. Bronson (Rodent Histopathology Core, Harvard Medical School, Boston, MA) for assistance with mouse histopathology and Dr Tanya Mayadas (Brigham and Women's Hospital, Boston, MA) for assistance regarding vascular permeability.

This work was supported by National Institutes of Health Grant CA42368 (to M.E.H.).

Authorship

Contribution: Y.T. and M.E.H. designed the studies and wrote the manuscript; Y.T., Q.L., A.R.K., M.E. and K.E. performed the research; A.R.K. contributed vital new reagents; and Y.T., A.R.K., M.E., K.E., S.J.T., and M.E.H. analyzed the data.

Conflict-of-interest disclosure: The authors declare no competing financial interests.

Correspondence: Martin E. Hemler, Dana-Farber Cancer Institute, 450 Brookline Ave, Boston, MA 02215-5450; e-mail: martin_hemler@dfci.harvard.edu.

References

1. Bogenrieder T, Herlyn M. Axis of evil: molecular mechanisms of cancer metastasis. *Oncogene.* 2003;22(42):6524-6536.
2. Al-Mehdi AB, Tozawa K, Fisher AB, et al. Intravascular origin of metastasis from the proliferation of endothelium-attached tumor cells: a new model for metastasis. *Nat Med.* 2000;6(1):100-102.
3. Berditchevski F, Odintsova E, Sawada S, Gilbert E. Expression of the palmitoylation-deficient CD151 weakens the association of alpha 3beta 1 integrin with the tetraspanin-enriched microdomains and affects integrin-dependent signalling. *J Biol Chem.* 2002;277(40):36991-37000.
4. Hemler ME. Tetraspanin proteins mediate cellular penetration, invasion and fusion events, and define a novel type of membrane microdomain. *Ann Rev Cell Dev Biol.* 2003;19:397-422.
5. Hemler ME. Tetraspanin functions and associated microdomains. *Nat Rev Mol Cell Biol.* 2005;6(10):801-811.
6. Martin F, Roth DM, Jans DA, et al. Tetraspanins in viral infections: a fundamental role in viral biology? *J Virol.* 2005;79(17):10839-10851.
7. Levy S, Shoham T. Protein-protein interactions in the tetraspanin web. *Physiology (Bethesda).* 2005;20:218-224.
8. Zöller M. Tetraspanins: push and pull in suppressing and promoting metastasis. *Nat Rev Cancer.* 2009;9(1):40-55.
9. Ikeyama S, Koyama M, Yamaoko M, Sasada R, Miyake M. Suppression of cell motility and metastasis by transfection with human motility-related protein (MRP-1/CD9) DNA. *J Exp Med.* 1993;177(5):1231-1237.
10. Tonoli H, Barrett JC. CD82 metastasis suppressor gene: a potential target for new therapeutics? *Trends Mol Med.* 2005;11(12):563-570.
11. Claas C, Seiter S, Claas A, et al. Association between rat homologue of CO-029, a metastasis-associated tetraspanin molecule and consumption coagulopathy. *J Cell Biol.* 1998;141(1):267-280.
12. Testa JE, Brooks PC, Lin JM, Quigley JP. Eukaryotic expression cloning with an antimetastatic monoclonal antibody identifies a tetraspanin

(PETA-3/CD151) as an effector of human tumor cell migration and metastasis. *Cancer Res.* 1999; 59(15):3812-3820.

13. Zijlstra A, Lewis J, Degryse B, Stuhlmann H, Quigley JP. The inhibition of tumor cell intravasation and subsequent metastasis via regulation of in vivo tumor cell motility by the tetraspanin CD151. *Cancer Cell.* 2008;13(3):221-234.
14. Sadej R, Romanska H, Kavanagh D, et al. Tetraspanin CD151 regulates transforming growth factor beta signaling: implication in tumor metastasis. *Cancer Res.* 2010;70(14):6059-6070.
15. Yauch RL, Berditchevski F, Harler MB, Reichner J, Hemler ME. Highly stoichiometric, stable and specific association of integrin alpha3beta1 with CD151 provides a major link to phosphatidylinositol 4-kinase and may regulate cell migration. *Mol Biol Cell.* 1998;9(10):2751-2765.
16. Sterk LM, Geuijen CA, van Den Berg JG, et al. Association of the tetraspanin CD151 with the laminin-binding integrins alpha3beta1, alpha6beta1, alpha6beta4 and alpha7beta1 in cells in culture and in vivo. *J Cell Sci.* 2002;115(pt 6):1161-1173.
17. Stipp CS, Hemler ME. Transmembrane-4-superfamily proteins CD151 and CD81 associate with alpha 3 beta 1 integrin, and selectively contribute to alpha 3 beta 1-dependent neurite outgrowth. *J Cell Sci.* 2000;113(pt 11):1871-1882.
18. Yáez-Mó M, Alfranca A, Cabañas C, et al. Regulation of endothelial cell motility by complexes of tetraspan molecules CD81/TAPA-1 and CD151/PETA-3 with alpha3beta1 integrin localized at endothelial lateral junctions. *J Cell Biol.* 1998; 141(3):791-804.
19. Sincock PM, Fitter S, Parton RG, et al. PETA-3/CD151, a member of the transmembrane 4 superfamily, is localised to the plasma membrane and endocytic system of endothelial cells, associates with multiple integrins and modulates cell function. *J Cell Sci.* 1999;112(pt 6):833-844.
20. Lammerding J, Kazarov AR, Huang H, Lee RT, Hemler ME. Tetraspanin CD151 regulates alpha6beta1 integrin adhesion strengthening. *Proc Natl Acad Sci U S A.* 2003;100(13):7616-7621.
21. Winterwood NE, Varzavand A, Meland MN, Ashman LK, Stipp CS. A critical role for tetraspanin CD151 in alpha3beta1 and alpha6beta4 integrin-dependent tumor cell functions on laminin-5. *Mol Biol Cell.* 2006;17(6):2707-2721.
22. Takeda Y, Kazarov AR, Butterfield CE, et al. Deletion of tetraspanin Cd151 results in decreased pathologic angiogenesis in vivo and in vitro. *Blood.* 2007;109(4):1524-1532.
23. Dlugosz AA, Glick AB, Tennenbaum T, Weinberg WC, Yuspa SH. Isolation and utilization of epidermal keratinocytes for oncogene research. *Methods Enzymol.* 1995;254:3-20.
24. Ye Z, Shi M, Chan T, et al. Engineered CD8(+) cytotoxic T cells with fiber-modified adenovirus-mediated TNF-alpha gene transfection counteract immunosuppressive interleukin-10-secreting lung metastasis and solid tumors. *Cancer Gene Ther.* 2007;14(7):661-675.
25. Grundy MA, Zhang T, Sentman CL. NK cells rapidly remove B16F10 tumor cells in a perforin and interferon-gamma independent manner in vivo. *Cancer Immunol Immunother.* 2007;56(8):1153-1161.
26. Sheng KC, van Spriel AB, Gartlan KH, et al. Tetraspanins CD37 and CD151 differentially regulate Ag presentation and T-cell co-stimulation by DC. *Eur J Immunol.* 2009;39(1):50-55.
27. Barnhill RL. The biology of melanoma micrometastases. *Recent Results Cancer Res.* 2001;158: 3-13.
28. Cowin AJ, Adams D, Geary SM, et al. Wound healing is defective in mice lacking tetraspanin CD151. *J Invest Dermatol.* 2006;126(3):680-689.
29. Lee TH, Avraham HK, Jiang S, Avraham S. Vascular endothelial growth factor modulates the transendothelial migration of MDA-MB-231 breast cancer cells through regulation of brain microvascular endothelial cell permeability. *J Biol Chem.* 2003;278(7):5277-5284.
30. Dvorak HF. Vascular permeability factor/vascular endothelial growth factor: a critical cytokine in tumor angiogenesis and a potential target for diagnosis and therapy. *J Clin Oncol.* 2002;20(21): 4368-4380.
31. Zachary I. VEGF signalling: integration and multitasking in endothelial cell biology. *Biochem Soc Trans.* 2003;31(pt 6):1171-1177.
32. Issbrücker K, Marti HH, Hippenstiel S, et al. p38 MAP kinase–a molecular switch between VEGF-induced angiogenesis and vascular hyperpermeability. *FASEB J.* 2003;17(2):262-264.
33. Nakashima Y, Yano M, Kobayashi Y, et al. Endostatin gene therapy on murine lung metastases model utilizing cationic vector-mediated intravenous gene delivery. *Gene Ther.* 2003;10(2):123-130.
34. Barreiro O, Yanez-Mo M, Sala-Valdes M, et al. Endothelial tetraspanin microdomains regulate leukocyte firm adhesion during extravasation. *Blood.* 2005;105(7):2852-2861.
35. Engbring JA, Kleinman HK. The basement membrane matrix in malignancy. *J Pathol.* 2003; 200(4):465-470.
36. Oka H, Emori Y, Hayashi Y, Nomoto K. Breakdown of Th cell immune responses and steroidogenic CYP11A1 expression in CD4+ T cells in a murine model implanted with B16 melanoma. *Cell Immunol.* 2000;206(1):7-15.
37. Paget C, Mallevaey T, Speak AO, et al. Activation of invariant NKT cells by toll-like receptor 9-stimulated dendritic cells requires type I interferon and charged glycosphingolipids. *Immunity.* 2007; 27(4):597-609.
38. Wright MD, Geary SM, Fitter S, et al. Characterization of mice lacking the tetraspanin superfamily member CD151. *Mol Cell Biol.* 2004;24(13): 5978-5988.
39. Yang XH, Flores LM, Li Q, et al. Disruption of laminin-integrin-CD151-focal adhesion kinase axis sensitizes breast cancer cells to ErbB2 antagonists. *Cancer Res.* 2010;70(6):2256-2263.
40. Yang XH, Richardson AL, Torres-Arzayus MI, et al. CD151 accelerates breast cancer by regulating alpha 6 integrin functions, signaling, and molecular organization. *Cancer Res.* 2008;68(9): 3204-3213.
41. Barreiro O, Zamai M, Yanez-Mo M, et al. Endothelial adhesion receptors are recruited to adherent leukocytes by inclusion in preformed tetraspanin nanoplatforms. *J Cell Biol.* 2008;183(3):527-542.
42. Rebhun RB, Cheng H, Gershenwald JE, et al. Constitutive expression of the alpha4 integrin correlates with tumorigenicity and lymph node metastasis of the B16 murine melanoma. *Neoplasia.* 2010;12(2):173-182.
43. Vitolo D, Ciocci L, Deriu G, et al. Laminin alpha2 chain-positive vessels and epidermal growth factor in lung neuroendocrine carcinoma: a model of a novel cooperative role of laminin-2 and epidermal growth factor in vessel neoplastic invasion and metastasis. *Am J Pathol.* 2006;168(3):991-1003.
44. Stipp CS. Laminin-binding integrins and their tetraspanin partners as potential antimetastatic targets. *Expert Rev Mol Med.* 2010;12:e3.
45. Weis SM, Lindquist JN, Barnes LA, et al. Cooperation between VEGF and beta3 integrin during cardiac vascular development. *Blood.* 2007; 109(5):1962-1970.
46. Shi GM, Ke AW, Zhou J, et al. CD151 modulates expression of matrix metalloproteinase 9 and promotes neoangiogenesis and progression of hepatocellular carcinoma. *Hepatology.* 2010;52(1): 183-196.
47. Sugiura T, Berditchevski F. Function of $\alpha 3\beta 1$-tetraspanin protein complexes in tumor cell invasion. Evidence for the role of the complexes in production of matrix metalloproteinase 2 (MMP-2). *J Cell Biol.* 1999;146(6):1375-1389.
48. Itoh T, Tanioka M, Yoshida H, et al. Reduced angiogenesis and tumor progression in gelatinase A-deficient mice. *Cancer Res.* 1998;58(5):1048-1051.
49. Hiratsuka S, Nakamura K, Iwai S, et al. MMP9 induction by vascular endothelial growth factor receptor-1 is involved in lung-specific metastasis. *Cancer Cell.* 2002;2(4):289-300.
50. Camerer E, Qazi AA, Duong DN, et al. Platelets, protease-activated receptors, and fibrinogen in hematogenous metastasis. *Blood.* 2004;104(2): 397-401.